INTERNATIONAL JOURNAL OF AUTOMOTIVE AND MECHANICAL ENGINEERING (IJAME)
ISSN: 2229-8649 e-ISSN: 2180-1606
VOL. 18, ISSUE 2, 8833 – 8844
DOI: https://doi.org/10.15282/ijame.18.2.2021.21.0677

ORIGINAL ARTICLE

Sound Intensity Mapping on Single Cylinder Direct Injection Diesel Engine with The Application of Palm Oil Methyl Ester Biodiesel

J.M. Zikri[1], M.S.M. Sani[1,2*] and A. Abdul Adam[2]

[1]Advanced Structural Integrity & Vibration Research, Faculty of Mechanical & Automotive Engineering Technology, Universiti Malaysia Pahang, 26600 Pekan, Pahang, Malaysia

[2]Automotive Engineering Centre, Universiti Malaysia Pahang, 26600 Pekan, Pahang, Malaysia

ABSTRACT – The utilisation of biodiesel nowadays has become familiar with rapid production types of biodiesel in order to replace the dependency on the fossil fuel parallel to the implementation of green technology that emphasises the products to be more environmental-friendly. Nevertheless, the emerges of various kinds of biodiesel cannot be simply used, despite using the biodiesel does not need any major modification on the engine; it still needs a few analyses that must be done to determine whether it will give advantages or disadvantages. Therefore, this research was carried out to investigate the effect of using palm oil methyl ester (POME) biodiesel on the engine in terms of noise emission. The sound intensity mapping method was used to indicate the effectiveness of the biodiesel by identifying the noise radiation. Along with the mapping, the sound power level (SPL) is also being obtained to provide a clear comparison between the parameters. Generally, switching up the engine speed and load increased the sound power level. Based on the results obtained related to the SPL, the intensity mapping tends to show a higher colour-coded in the noise source image for the higher engine speed and load setup. It was found that the engine speed and load give a significant contribution to noise emission produced by the engine, and it can be inferred that this method can be utilised to accomplish the noise emission analysis.

ARTICLE HISTORY
Received: 10th Dec 2020
Revised: 17th July 2021
Accepted: 27th July 2021

KEYWORDS
Biodiesel;
Noise emission;
Sound intensity mapping;
Sound power level;
Diesel engine

INTRODUCTION

Considering the power delivered by the engine with the low consumption of fuel may differ depending on the mechanism of the engine. Due to this reason, the diesel engine was profoundly known as a better solution to satisfy all the requirements. Commonly characterised by its high thermal efficiency, low fuel consumption and high sustainability have been widely used compared to gasoline engines [1]. The mechanism of the diesel engine has allowed the engine to produce high power through the great compression between air-fuel mixture that ignited when it comes to specific fire points [2]. Despite all the advantages of the diesel engine, there are also disadvantages that cannot be neglected. The most significant is the engine suffered from high emissions of particulate matter (PM) and nitrogen oxides (NOx) that can cause environmental pollution and have an adverse effect on human health [3]. Being added by health experts, the formation of acid rain, ozone layer depletion and low vision can also happen due to the pollution produced by the combustion of diesel engines. The mitigation efforts to reduce these problems is arduous due to their trade-off characteristic [4–7].

In different circumstances, the heavy usage of petroleum-based fuel has led to the depletion of sources of fossil fuel since diesel fuel is produced from a non-renewable source. It was considered a major issue due to the diminishment of sources, and it was reported that the remaining sources only could cover up demand up to approximately 50 years [8–10]. It takes millions of years to get the fossil fuels before they can be processed to produce the fuel. Hence, it has grown an intense interest for the researcher to find a replacement and an alternative substance to reduce the dependency on fossil fuel [11]. Among all the inventions, biodiesel seems to be the best substitution for conventional fuel by showing positive results on sustaining fuel production and reducing the emissions of CO, PM and HC [12–15]. Biodiesel is one of the renewable sources fuel, which can be produced through several processes from vegetable oils, animal fats and waste products, also known as biodegradable, that can deliver almost similar energy to fossil fuels [16]. Among all of the production methods, the most attractive was transesterification, where the vegetable oil or animal fats reacted with the alcohol in the presence or without the catalyst to form an ethyl or methyl ester. They either can be used directly or blended with the petroleum-based fuel up to 20% of the blending ratio without a need for major modification on the engine [17–21].

*CORRESPONDING AUTHOR | M.S.M. Sani | ✉ mshahrir@ump.edu.my

RELATED WORKS

Nevertheless, the usage of biodiesel still needs to undergo a few analyses, including the noise emission, to determine its capability in sustaining the performance in the engine. To investigate the combustion noise radiated by the engine, Siavash et al. [22] has conducted an experimental study with the neat diesel and biodiesel usage with the increment of 5% blending ratio up to 30%. They found out that the B10 tends to show the lowest sound pressure level (SPL) due to the lower combustion pressure. On the contrary, a work that has been done by Chiatti et al. [23] presented that the B10 of waste cooking oil (WCO) gives the highest values of noise index (NI) while B40 represents the lowest with the load condition. The author highlighted that the higher the volume of biodiesel, the lower the magnitude of NI and this were related to the ignition delay and the rate of pressure rise (RoPR) that varied accordingly. While in a study by Yıldırım et al. [24], the pure WCO (B100) usage has demonstrated a lower level of noise amplitude, and this was attributed to the higher cetane number of the biodiesel that improving the combustion in the engine.

In a different study, Zhen et al. [25] tested the pure rapeseed oil biodiesel (B100) together with B50 as a fuel in the direct injection diesel engine. It seems that the fuel properties of rapeseed oil have driven to the increment of SPL, as can be noticed where both of the B50 and B100 generates higher SPL compared to the diesel. This can be explained by the higher peak pressure and heat release rate (HRR) of the biodiesel blend. Similarly, Patel et al. [26] indicated that the B20 and B100 of rapeseed biodiesel generated higher external noise. However, the combustion noise for all biofuels tested somehow shows an interesting side of the biodiesel usage where it could attenuate from 0.25 to 7 dB(A) lower than the diesel. The author stated that this happened due to the lower maximum HRR. Previously, the same author [27] has utilised the karanja biodiesel with the same proportions, which is B20 and B100. They have found out that in the combustion noise, the B20 was the highest, and the B100 was the lowest as the B20 produces the higher HRR that was consequently increasing the RoPR. Meanwhile, in the overall noise level, the B100 shows the highest level of noise, and this was associated with the noise generated by the engine's mechanical components.

The sunflower and canola biodiesel fuel in the diesel engine has been carried out by Uludamar et al. [28] with an increment of 20% up to 100% of blending ratio. It can be stressed out that biodiesel usage averagely could reduce the SPL compared to diesel as the vibration of engine block decreases. Hence, proving that the noise and the vibration in diesel engine was in linear-relationship. Identically, similar results were reported by Yildizhan et al. [29] in their study by using the same types of biodiesel. They have found that the biodiesel blends could cause a decrement in SPL due to the lower vibration of the engine body. As one of the methods to enhance the quality of the fuel mixture, Çelebi et al. [30] inducted the natural gas that highly contains methane with the flow rate of 5, 10 and 15 ℓ/m. They have concluded that except for the low engine speed (1200 rpm), the conventional diesel produces higher SPL. It is notable that the improved properties of the fuel mixture have contributed to the reduction in the noise level by enhancing the combustion process in the cylinder. The same improvements were made by Uludamar et al. [31] to sunflower and canola biodiesel with the addition of hydrogen by 3 and 6 ℓ/m. Slightly further decrement can be noticed for both of the flow rates. Generally, the addition of hydrogen can lower the SPL due to the differences in the combustion characteristics.

Patel et al. [32] have considered the jatropha biodiesel to be used in the single-cylinder direct injection diesel engine with the volume of 20 % and 100%. They have listed several of their findings where the combustion noise generated by the B20 was the highest for most load conditions while the least was obtained by B100. The increment of maximum HRR has led to the increment of the combustion noise. As for the overall noise level, the results revealed that a high portion of biodiesel gives a louder operation of the mechanical components, consequently influencing the overall noise level. Meanwhile, a study by Ravi et al. [33] has shown that the smaller fraction of biodiesel content tends to produce a lower noise level as the B30 of Jatropha biodiesel gives the lowest noise by 94.9 dB. The author also highlighted that with the increment of biodiesel content from 10 % to 30 %, smoother combustion takes place.

Based on the past studies, the effect of biodiesel is still under observation, and improvisation can be made through an appropriate blending ratio with the diesel fuel in order to achieve a minimum level of noise. It can be summarised, different blends ratio can attenuate the noise accordingly to the combustion quality that is strongly influencing the vibration level and consequently affecting the noise level produced by the engine. Hence, in this paper, the noise emission analysis was carried out on a single-cylinder compression ignition engine in terms of sound power level (SPL) as well as sound intensity mapping by using a diversity blending ratio of POME.

METHOD AND MATERIALS

Compression-Ignition Engine

The diesel engine that has been used in this study was manufactured by YANMAR and modelled as TF 120 M which is a horizontal single-cylinder, 4-stroke, water-cooled and direct injection. In order to give the real application such as an engine that mounted in a vehicle, the engine was coupled with an eddy current dynamometer that applied a load to the engine by medium and high level. The study was conducted using two speeds representing low and high speeds where the low speed was at 1200 rpm, and the high speed was at 2160 rpm. Figure 1 and Table 1 illustrated the engine and its specification.

Figure 1. YANMAR TF120 M diesel engine.

Table 1. YANMAR TF120 M diesel engine specification.

Specifications	YANMAR TF 120M
No of cylinder	1
Cylinder bore × stroke (mm)	92×96
Displacement, cc	0.638
Cooling system	Hopper/radiator
Dimensions: length × width × height (mm)	695×348.5×530
Compression ratio	17.7

Bump Test

The bump test is a method that can be used to determine the dynamic properties of the engine, and this test was intended to obtain the natural frequency in order to avoid the resonance effect in the rotational frequency. By giving forces through the impact hammer as the input and readings from an accelerometer as the output, the frequency response function of the engine can be determined. Choosing the right size of impact hammer, the type of hammer tip and triggered point were considerable factors since they could contribute to inaccurate results. As the size and material of the engine being identified, the big impact hammer with a hard tip was used to trigger the best point (point 1), which was chosen based on the coherence analysis. The impact hammer and the triggered point are shown in Figure 2(a) and 2(b).

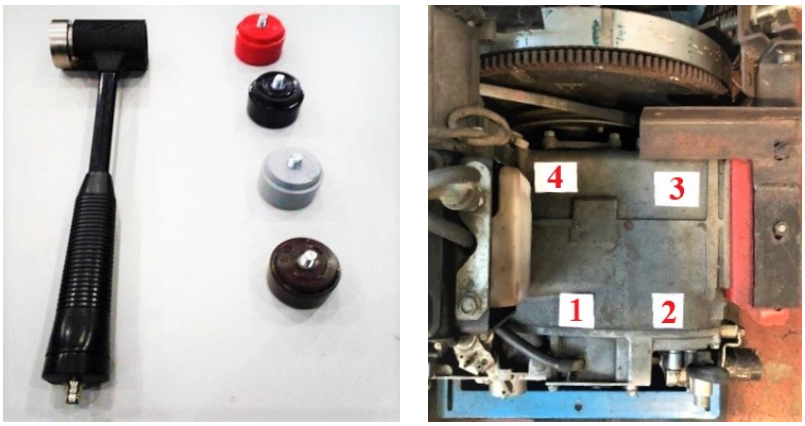

(a) (b)

Figure 2. (a) Big impact hammer and, (b) trigger points.

Preparation of Fuel

The tested fuel in the engine was prepared right before the experiment and measurement. This was purposely done to ensure the best quality of fuel, especially when involving the biodiesel, and further, the re-blend process was done for the leftover fuel to avoid an immature fuel mixture. Together with pure diesel, there are three types of fuel mixtures which are B10 and B20 of POME, that follows the blended fuel standard ASTM D7467 specifications by their properties. For the blending process, the digital overhead stirrer (IKA RW 20 digital) has been used with 1000 rpm speed for 30-40 minutes instead of an ultrasonic processor since there is no addition of other substances. A visual quality indicator was used to determine the completeness of the mixing process based on the clarity of the mixture where the well-blend mixture shows clear-visual.

Noise Emission Measurement

In the process of collecting data, each measurement was done averagely by 3 seconds for each grid after a steady-state condition was achieved and maintained through monitoring the digital control centre of the engine. There are two analyses of noise emission involved: noise intensity mapping. This method helps determine the noise hotspots quickly and recognises the pattern of noise intensity in the noise source in such no time. Hence, reducing the time-consumed noise and identification cost. Along with the magnitude, the direction of the energy in the sound field also can be obtained. The second analysis is the sound power level which is used to identify the difference in the noise level. Both of the analyses use the Brüel & Kjær Hand-held Analyzer Types 2270 together with the sound intensity probe, and Measurement Partner Suite analysing software. The calibration phase for the transducer is needed to prevent unprecise and inaccurate data. Hence, in this process, both microphones were calibrated using B&K Type 4231 sound calibrator.

Table 2. Handheld analyser type 2270 specifications.

Specifications	Type 2270
Input	dual channels
Display	large, high-resolution, touch-sensitive colour screen
Hardware interface	integral digital camera for documentation and reference
Measurement range	dynamic range in excess of 123 dB(A) 0.5 Hz – 20 kHz broadband linear range
Measurement status	red, yellow and green LEDs show measurement status
Quality indicator	'smiley' quality indicators with hints and warnings

Noise Source Setup

Before start measuring the data, the design of the noise source was set in the handheld analyser, where the dimension of the noise source was used to determine the number of grids. In this study, the 6×6 grid was used in order to follow the ISO 9614-3, which set that each segment must be in 0.1 m. The gridding noise source is pictured in Figure 3.

Figure 3. Gridding of a noise source.

Sound Intensity Measurement Formulation

It is reported by Crocker and Arenas[34] that the most efficient sound intensity measurement principle employed two closely spaced pressure microphones[35] where the particle velocity was obtained using Euler's relation:

$$\nabla p(t) + \rho \frac{\partial u(t)}{\partial t} = 0 \tag{1}$$

or

$$u_r^{(e)}(t) = -\frac{1}{\rho} \int_{-\infty}^{t} \frac{p_2(\tau) - p_1(\tau)}{\Delta r} d\tau \tag{2}$$

where, p_1 and p_2 are the sound pressure signals from the two microphones, Δr is the microphone separation distance, and τ is a dummy time variable. The caret indicates the finite difference estimate obtained from the two-microphone approach. The sound pressure at the centre of the probe is estimated from:

$$p^{(e)}(t) = \frac{p_1(t) + p_2(t)}{2} \tag{3}$$

and the time-averaged sound intensity component in the axial direction is, from Eq.(2), (3), and (4).

$$I = (p(t)u(t))_t \tag{4}$$

$$I_r^{(e)} = \frac{1}{2\rho\Delta r}([p_1(t) + p_2(t)] \int_{-\infty}^{t} [p_1(\tau) - p_2(\tau)]d\tau) \tag{5}$$

Some of the commercial sound intensity analysers use Eq.(5) to measure the intensity in 1/3 octave frequency bands and there is also another way to measure the intensity by obtaining the imaginary part of the cross-spectrum G_{12} between the two microphone signals using dual-channel FFT analyser, which derived by Fahy and Chung [36, 37].

$$I_r^{(e)}(\omega) = -\frac{1}{\omega\rho\Delta r} Im\{G_{12}(\omega)\} \tag{6}$$

RESULTS AND DISCUSSION

Bump Test

Since this study focuses on low frequency, hence the natural frequency was considered up to 100 Hz. From the test that was carried out, it can be observed in Figure 4 that the natural frequencies happened at 24 Hz, 30 Hz, 46 Hz, 70 Hz and 84 Hz, with the lowest magnitude almost 0.001 g/N and the highest close to 0.004 g/N. All frequencies obtained were avoided by using the rule of thumb to decide the rotational speed frequency in order to prevent resonance effects.

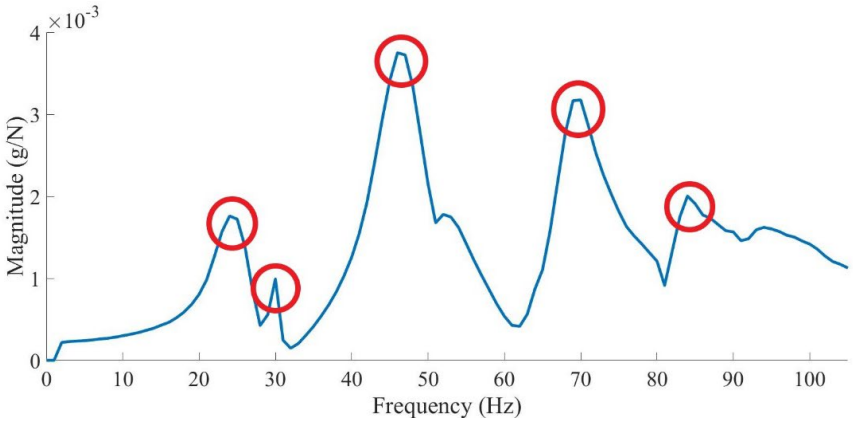

Figure 4. Natural frequencies in the diesel engine.

Sound Intensity Mapping

The sound intensity mapping results are shown in the colour-codes for each grid where it indicates the level of the intensity produced by the noise source. Table 3 provides the components included in the test rig based on the grid and the colour codes for the mapping. Precisely, this mapping can only be compared with the other mapping through the intensity of colour codes and the pattern to gain a better understanding of the mechanism of noise generated by the noise source. Therefore, the SPL values are needed to identify the differences in noise level between each fuel.

Speed without load

As can be seen in Figure 5(a), the pure diesel D100 tends to show a brighter colour in several points, which represents a higher intensity level compared to the B10 and B20 in Figure 5(b) and 5(c). By focussing on the sub-components of the engine in all fuels, the mapping clearly shows that the centre of the engine where the crankshaft allocated was the constant one that represents a higher level of intensity. This may happen due to the forces associated with the crankshaft, bearing clearances, element deformation and friction, which generates the mechanical noise [38–40]. The other component that shows similar results was the radiator where the noise at this location comprises of the radiator, belting and the pulley, hence it can be agreed with a finding by Razak et al. [41], which found that the radiator system also contributes to the noise radiation by the engine.

As for the high rotational speed, it can be observed that most grids of the noise source were covered up by the brighter colour code, as can be referred to Figure 5(d) to 5(f). When using a higher engine speed, the results tend to show a higher intensity level, and it was proven that the engine speed is strongly related to the noise generated by the engine where the higher the engine speed, the higher the noise level due to the increase of combustion strokes and piston blows per the unit time [42–45]. It is noticeable that both D100 and B20 produce high-intensity levels at the right side of the engine where the crank-link is operated while B10 has a smoother operation, which happens due to lower heat release rate (HRR) of B10 at a higher speed [42].

Table 3. Components of the diesel engine.

Points	Components	Mapping colour indicator
1 - 2	fuel overflow	
3 - 6	engine mounting	
7 - 10	engine base	
11 - 12	fuel overflow	
13	intake manifold	
14	cylinder head	
15	piston	
16	connecting rod	
17	crankshaft	
18 - 21	crankcase and belting	
22 - 23	radiator base	
24	lower intake and exhaust pipe	
25	middle intake pipe	
26 - 28	radiator	
29 - 33	flywheel and dynamometer	
34 - 35	top radiator	
36	upper intake pipe	

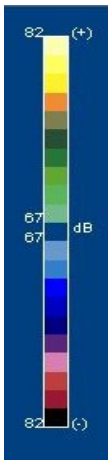

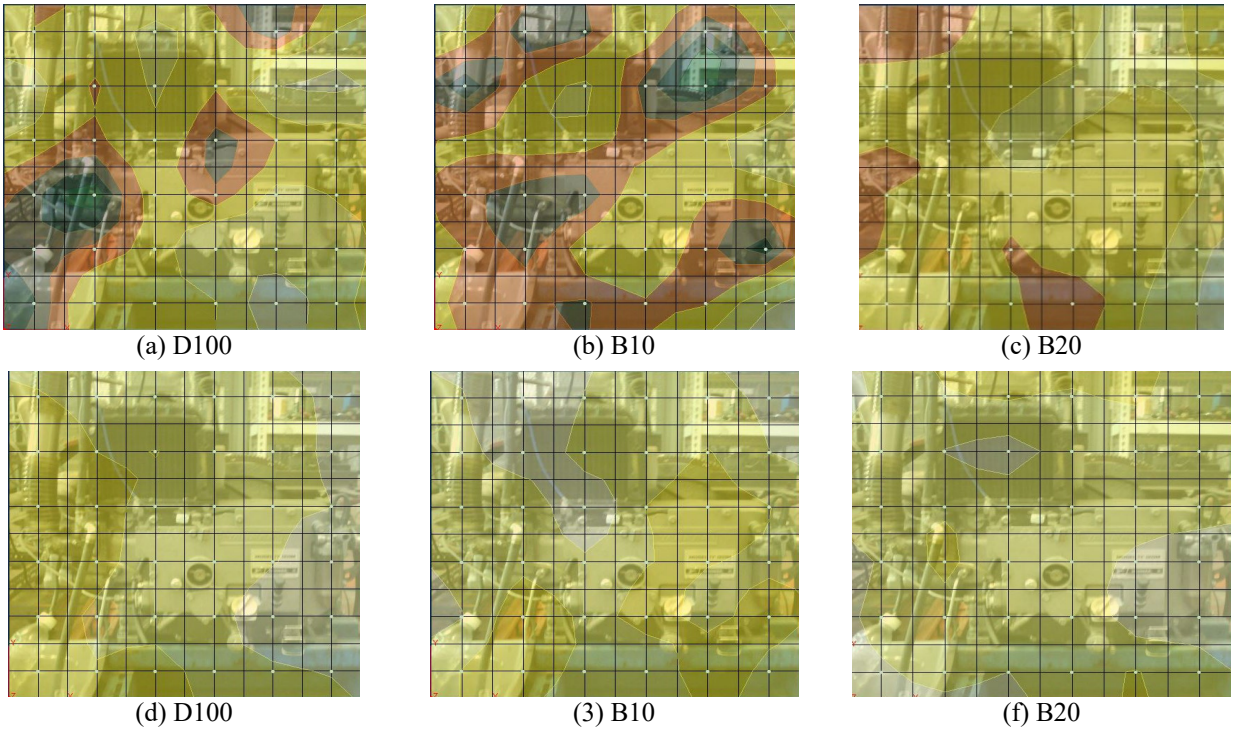

(a) D100 (b) B10 (c) B20

(d) D100 (3) B10 (f) B20

Figure 5. Sound intensity mapping without load (0 Nm) at (a),(b),(c) low speed and (d),(e),(f) high speed.

Speed with medium load

Figure 6(a) to 6(c) illustrates the mapping for each fuel with the presence of a medium load at 14 Nm and low rotational speed. It can be highlighted that the B20 mapping was nominated by the high-intensity level compared to D100 and B10 with the application of load, especially at the centre of the engine and the engine mounting area. Once again, the enhanced combustion quality of B10 and B20 blends where the shorter ignition delay (ID) could possibly owe to lower pressure inside the cylinder [46–48]. In contrast to B20, B10 shows a remarkable reduction in noise emitted by the intake manifold, cylinder head and crank-link compared to D100 that can be explained due to the best viscosity level of blend that influencing the start of injection and injection pressure [49, 50]. Up to this point, the B10 blend was able to produce lower intensity level.

Nevertheless, when the medium load was applied at the high engine speed, the D100 appeared to be the lowest intensity level in several points near the cylinder head area (left side of mapping), with the B10 that shows a considerably lower level compared to the B20. Still, in this condition, the area that is supposed to show a concentrated intensity located on the top right of the mapping, B10, generated the lowest level, as can be seen in Figure 6(d) to 6(f). Where the improved cetane number (CN) of B10 may be a considerable factor for the reduction of the loudness of engine noise [51], and this loudness was reported to be highly correlated with the SPL [52]. On top of that, the B20 blend present a constant level of intensity except for the right side, where the flywheel and dynamometer contribute the most noise emission together with

the crank operation. This may attribute to the mechanical-induced energy that were affected by the higher kinematic viscosity and density of the B20 [53, 54].

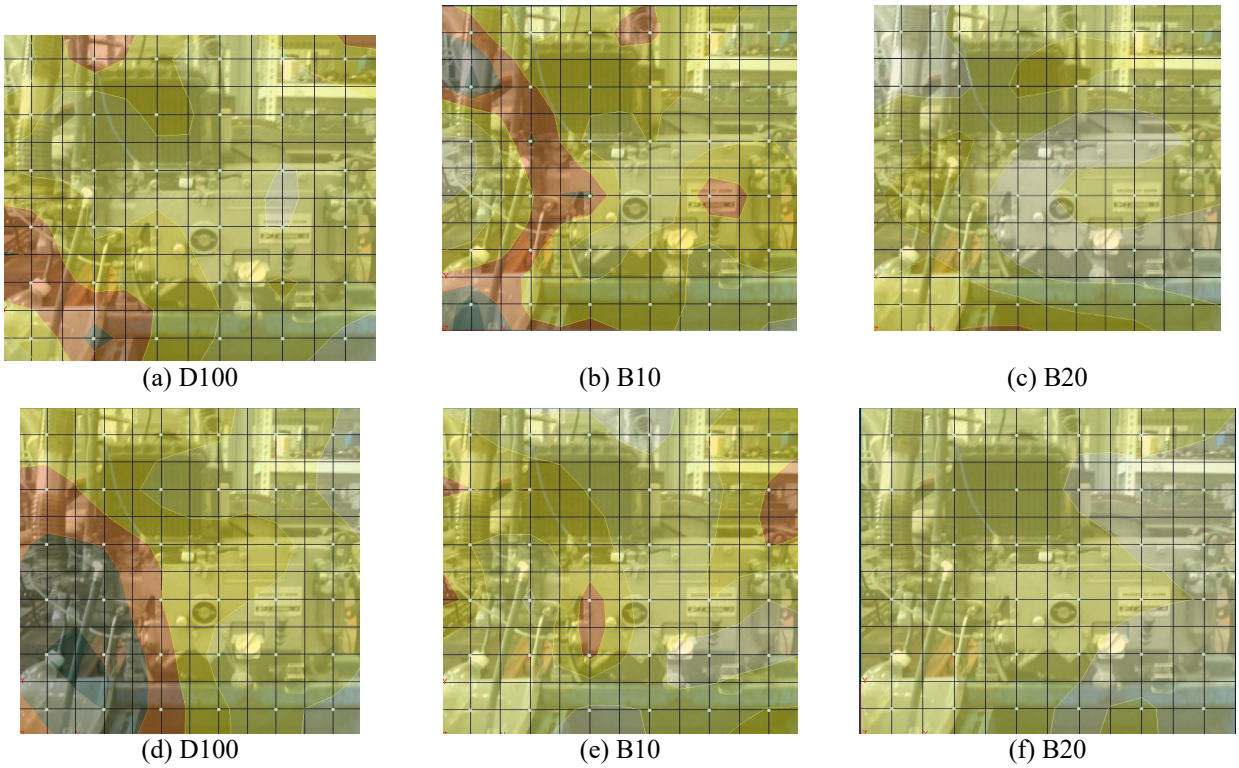

(a) D100 (b) B10 (c) B20

(d) D100 (e) B10 (f) B20

Figure 6. Sound intensity mapping for medium load of 14 Nm at (a),(b),(c) low speed and (d),(e),(f) high speed.

Speed with high load

However, when the high load was given to the engine, surprisingly, the B10 blend develops the highest intensity level on the right side, which concentrated on the dynamometer area and mechanical noise compared to other fuel, as displayed in Figure 7(a) to 7(f). This significant increase may be due to greater thermal efficiency that helps to develop higher noise levels [42]. Ironically, the B20 blend that usually nominates the highest level of intensity becomes the lowest in the overall noise level. It was revealed that the fuel properties of the blend might be more convenient with this parameter.

As demonstrated in Figure 7(a), when the high rotational speed and high load were used, once again, D100 proves that it still produces the lowest intensity level in the left side area where the intake manifold, exhaust pipe and cylinder head located with the presence of load. Interestingly, the mapping reflects the increment of load could increase the noise level at the valve closures [55]. On the contrary, the B20 blend was found to be the highest at the high engine speed whereas, at the low engine speed, it was the lowest. It can be noted how the engine speed can affect the noise emission level produced by the engine since the fuel mixture process deteriorated that resulting in more abrupt HRR and consequently higher noise level [56]. Based on the intensity mapping results, it can be concluded that during the high engine speed and high load, the D100 fuel characteristics could tolerate the lower intensity level at several components. Along with the pattern of the mapping for all fuel tested, the components that major contributed to the noise generation were found to be the crankshaft, connecting rod and flywheel section.

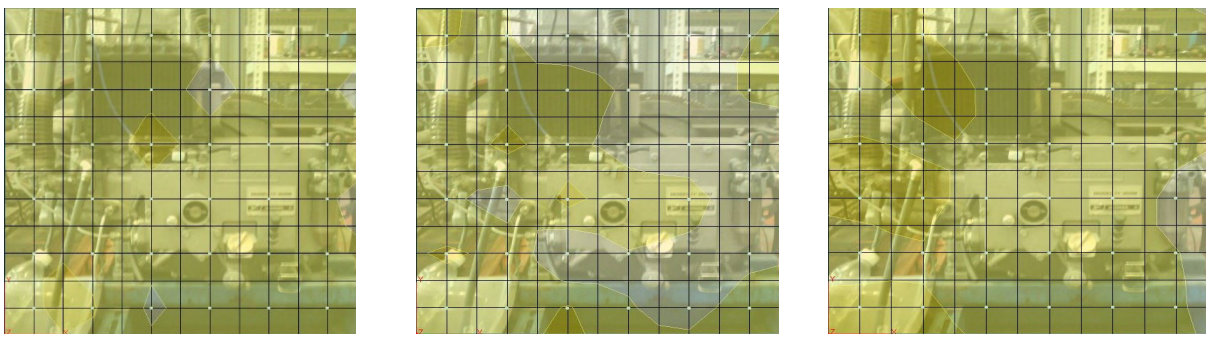

(a) D100 (b) B10 (c) B20

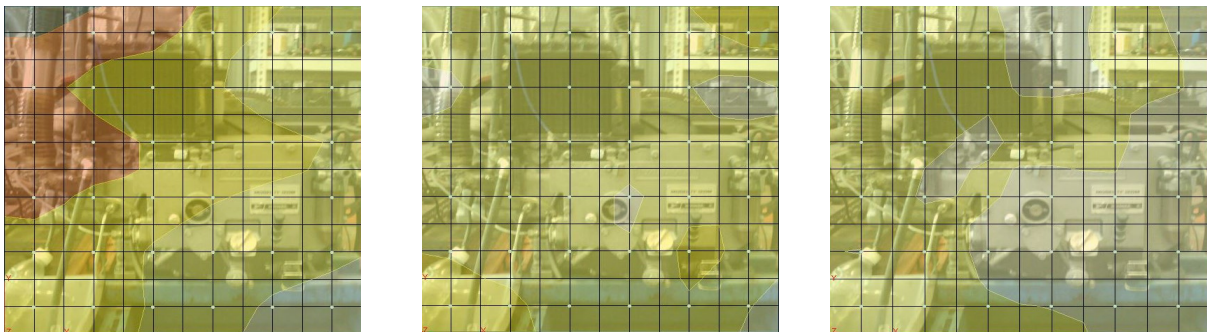

(d) D100 (e) B10 (f) B20

Figure 7. Sound intensity mapping for high load of 28 Nm at (a),(b),(c) low speed and (d),(e),(f) high speed.

Sound Power Level

Regarding the SPL for all points, the values were plotted in the graph by using MATLAB to provide a clearer image for interpretation of data to show the difference in noise level for each type of fuel used. Each fuel's data were plotted together in a single graph according to the same parameter.

Low speed without load

From Figure 8(a) data, parallel to the intensity level produced by the engine, the SPL for D100 shows the highest for overall noise level. Nevertheless, D100 represents the lowest SPL in the cylinder head area with a difference of approximately 4 dB compared to B10 and B20. As explained, the higher kinematic viscosity and density of biodiesel blends have influenced the process of injection in the engine [57]. In spite of that, both B10 and B20 have shown some improvements by the noise reduction in the engine mounting area, intake pipes and flywheel section. It can be discussed that the biodiesel blends were able to attenuate the air dynamic and mechanical noises produced by the engine [58].

Low speed with medium load

Based on the results presented earlier, it can be clarified that even the B20 intensity mapping tends to be more intense compared to D100. D100 tends to produce higher SPL in several components, as referred to in Figure 8(b), where an obvious gap was observed between B10 and B20 at the crankshaft, belting and radiator. It is also notable that the biodiesel usage was able to tolerate the presence of medium load where both of the blends produce lower levels at the flywheel and dynamometer location. The extra oxygen content of biodiesel that helps to the appropriate fuel combustion was the potential cause to reduce the noise generated by reducing the knocking tendency [59]. Additionally, the higher cetane number of biodiesels tend to prevent a longer ignition delay and stronger premixed combustion; hence it improved the combustion duration [60].

Low speed with high load

Figure 8(c) is quite revealing the variation results of SPL. Unlike the previous experimental setup, the B20 blend shows noteworthy mitigation of SPL, approximately around 3 dB compared to D100. At the same time, the rises of SPL in the B10 blend were contributed by the flywheel and dynamometer, as the incomplete combustion took placed due to the rich air-fuel mixture during high engine load [61]. It is visible that the trend has become more consistent with the increment of engine load. In spite of that, the highest SPL was generated by D100 at the radiator with a value of 93.09 dB. Similarly, Patel et al. [32] reported that the noise from the radiator was noisy and influenced the overall external noise level. Overall, D100 still nominated the noise level produced by almost 2/3 total points of high SPL in the current setup. With the high brake load applied to the low engine speed, it could be sum up that regardless of the types of noise induction, biodiesel usage has improved the noise characteristics of the engine by the better fuel properties.

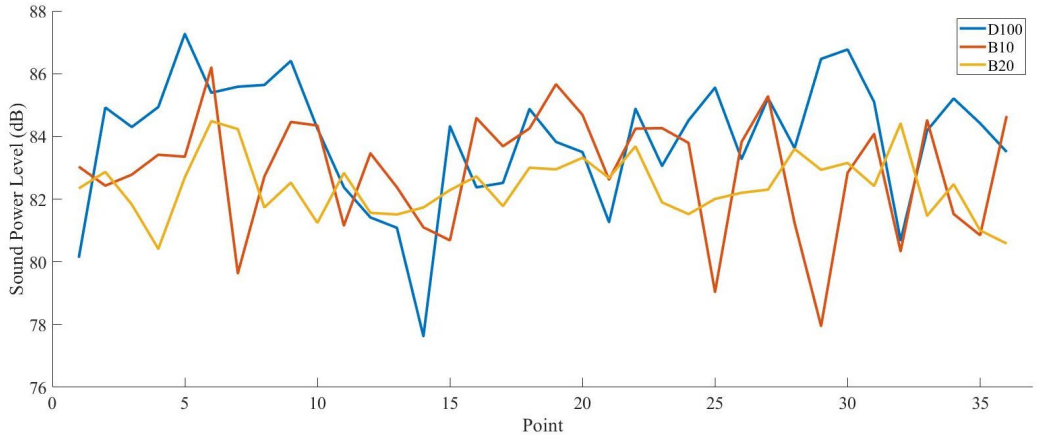

(a)

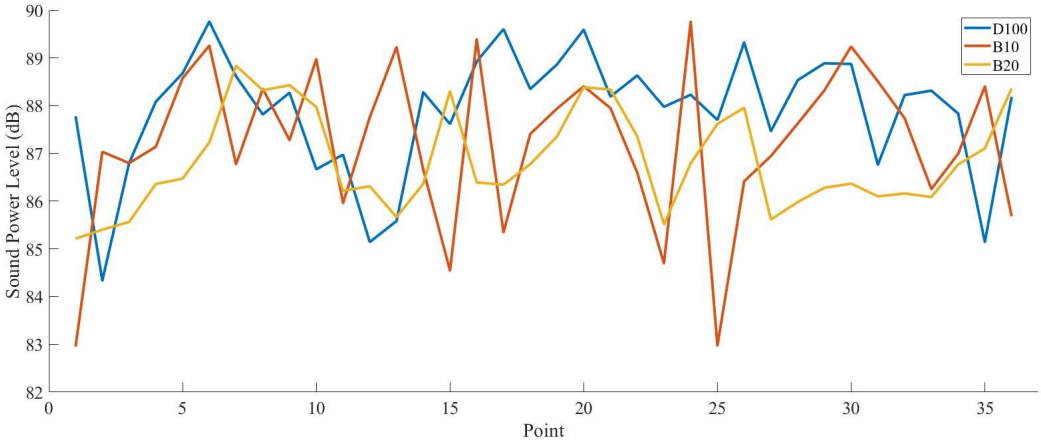

(b)

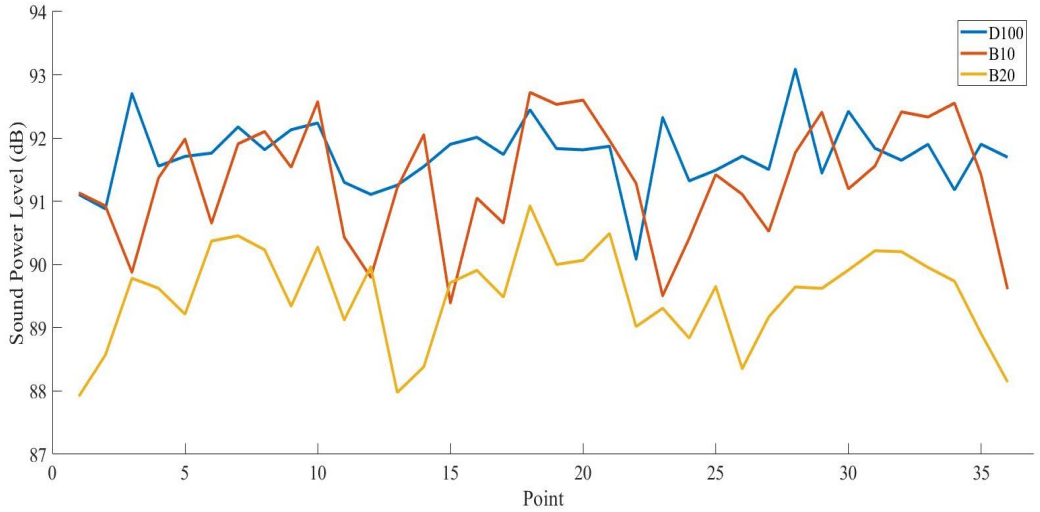

(c)

Figure 8. Low speed (a) without load (0 Nm), (b) with a medium load of 14 Nm. (c) with a high load of 28 Nm.

CONCLUSION

In conclusion, the following points emerged from the present investigation:

i. The engine speed and load were found to be the considerable factors that can cause an increment in the noise level through the excitation forces of the engine components.

ii. Different blend ratios that give different fuel properties play an important role to enhance the noise level. In this study, the B10 blend tends to be the most suitable fuel that can reduce the noise level at the engine mounting,

intake manifold and dynamometer area. In contrast, by the overall noise level, the B20 shows a persistent attenuation of noise.

iii. It is also notable that the baseline fuel could produce a low noise level at the intake manifold and cylinder head area when using high engine speed.

iv. The results of the present study also suggest that mechanical noise could be the obvious noise source other than combustion and random sources.

These findings provide that for future research where more blends of biodiesel or with an additive should be done in order to determine the most efficient substitution of fossil fuel in this new ecology system.

ACKNOWLEDGEMENT

The authors would like to thank the Universiti Malaysia Pahang for providing financial support under Internal Research grant PGRS 1903151 and laboratory facilities.

REFERENCES

[1] Park H, Shim E, Bae C. Improvement of combustion and emissions with exhaust gas recirculation in a natural gas-diesel dual-fuel premixed charge compression ignition engine at low load operations. Fuel 2019; 235: 763–774.

[2] Gill P, Soni SK, Kundu K. Comparative study of hemp and jatropha oil blends used as an alternative fuel in diesel engine. Agricultural Engineering International: CIGR Journal 2011; 13: 1–11.

[3] Agarwal AK, Gupta T, Kothari A. Particulate emissions from biodiesel vs diesel fuelled compression ignition engine. Renewable and Sustainable Energy Reviews 2011; 15: 3278–3300.

[4] Li G, Gu F, Wang T, et al. Investigation into the vibrational responses of cylinder liners in an IC engine fueled with biodiesel. Applied Sciences 2017; 7(7): 717.

[5] Huang H, Liu Q, Teng W, et al. Improvement of combustion performance and emissions in diesel engines by fueling n-butanol/diesel/PODE3–4 mixtures. Applied Energy 2018; 227: 38–48.

[6] Elsanusi OA, Roy MM, Sidhu MS. Experimental investigation on a diesel engine fueled by diesel-biodiesel blends and their emulsions at various engine operating conditions. Applied Energy 2017; 203: 582–593.

[7] Hwang J, Bae C, Patel C, et al. Investigations on air-fuel mixing and flame characteristics of biodiesel fuels for diesel engine application. Applied Energy 2017; 206: 1203–1213.

[8] Silitonga AS, Mahlia TMI, Kusumo F, et al. Intensification of Reutealis trisperma biodiesel production using infrared radiation: Simulation, optimisation and validation. Renewable Energy 2019; 133: 520–527.

[9] Ullah K, Ahmad M, Sofia, et al. Synthesis and characterisation of biodiesel from Aamla oil: A promoting non-edible oil source for bioenergy industry. Fuel Processing Technology 2015; 133: 173–182.

[10] Damanik N, Ong HC, Tong CW, et al. A review on the engine performance and exhaust emission characteristics of diesel engines fueled with biodiesel blends. Environmental Science and Pollution Research 2018; 25: 15307–15325.

[11] Krohn BJ, Fripp M. A life cycle assessment of biodiesel derived from the 'niche filling' energy crop camelina in the USA. Applied Energy 2012; 92: 92–98.

[12] Shan R, Lu L, Shi Y, et al. Catalysts from renewable resources for biodiesel production. Energy Conversion and Management 2018; 178: 277–289.

[13] Ali B, Yusup S, Quitain AT, et al. Synthesis of novel graphene oxide/bentonite bi-functional heterogeneous catalyst for one-pot esterification and transesterification reactions. Energy Conversion and Management 2018; 171: 1801–1812.

[14] Gebremariam SN, Marchetti JM. Economics of biodiesel production: Review. Energy Conversion and Management 2018; 168: 74–84.

[15] Arumugam A, Ponnusami V. Biodiesel production from Calophyllum inophyllum oil a potential non-edible feedstock: An overview. Renewable Energy 2019; 131: 459–471.

[16] Lokanatham R, Prof.Ravindranath K. Extraction and use of non-edible oils in bio-diesel preparation with performance and emission analysis on ci engine. International Journal of Engineering Research and Development 2013; 6: 35–45.

[17] Sander A, Antonije Košćak M, Kosir D, et al. The influence of animal fat type and purification conditions on biodiesel quality. Renewable Energy 2018; 118: 752–760.

[18] Rattanaphra D, Soodjit P, Thanapimmetha A, et al. Synthesis, characterisation and catalytic activity studies of lanthanum oxide from Thai monazite ore for biodiesel production. Renewable Energy 2019; 131: 1128–1137.

[19] Vardast N, Haghighi M, Dehghani S. Sono-dispersion of calcium over Al-MCM-41used as a nanocatalyst for biodiesel production from sunflower oil: Influence of ultrasound irradiation and calcium content on catalytic properties and performance. Renewable Energy 2019; 132: 979–988.

[20] Malhotra R, Ali A. 5-Na/ZnO doped mesoporous silica as reusable solid catalyst for biodiesel production via transesteri fi cation of virgin cottonseed oil. Renewable Energy 2019; 133: 606–619.

[21] Somnuk K, Soysuwan N, Prateepchaikul G. Continuous process for biodiesel production from palm fatty acid distillate (PFAD) using helical static mixers as reactors. Renewable Energy 2018; 131: 100–110.

[22] Siavash NK, Najafi G, Hasanbeigi R, et al. Acoustic analysis of a single cylinder diesel engine using biodiesel fuel blends. Energy Procedia 2015; 75: 893–899.

[23] Chiatti G, Chiavola O, Palmieri F. Vibration and acoustic characteristics of a city-car engine fueled with biodiesel blends. Applied Energy 2017; 185: 664–670.

[24] Yıldırım H, Çınar A. Vibration and noise depending on engine speed in a diesel engine fueled with biodiesel. In: 6th Europe Conference Renewable Energy System, Istanbul, Turkey; 25-27 Jun, 2018.

[25] Zhen D, Wang T, Gu F, et al. Combustion analysis of a CI engine with biodiesel blends based on vibro-acoustic measurement. In: 9th International Conference on Condition Monitoring and Machinery Failure Prevention Technologies 2012, London, UK, pp. 85-97; 2012

[26] Patel C, Tiwari N, Agarwal AK. Experimental investigations of Soyabean and Rapeseed SVO and biodiesels on engine noise,

vibrations, and engine characteristics. Fuel 2019; 238: 86–97.
[27] Patel C, Agarwal AK, Tiwari N, et al. Combustion, noise, vibrations and spray characterisation for Karanja biodiesel fuelled engine. Applied Thermal Engineering 2016; 106: 506–517.
[28] Uludamar E, Tosun E, AydIn K. Experimental and regression analysis of noise and vibration of a compression ignition engine fuelled with various biodiesels. Fuel 2016; 177: 326–333.
[29] Yildizhan Ş, Uludamar E, Özcanli M, et al. Evaluation of effects of compression ratio on performance, combustion, emission, noise and vibration characteristics of a VCR diesel engine. International Journal of Renewable Energy Research 2018; 8(1): 90-100.
[30] Çelebi K, Uludamar E, Tosun E, et al. Experimental and artificial neural network approach of noise and vibration characteristic of an unmodified diesel engine fuelled with conventional diesel, and biodiesel blends with natural gas addition. Fuel 2017; 197: 159–173.
[31] Uludamar E, Yildizhan Ş, Aydin K, et al. vibration, noise and exhaust emissions analyses of an unmodified compression ignition engine fuelled with low sulphur diesel and biodiesel blends with hydrogen addition. International Journal of Hydrogen Energy 2016; 41: 11481–11490.
[32] Patel C, Lee S, Tiwari N, et al. Spray characterisation, combustion, noise and vibrations investigations of Jatropha biodiesel fuelled genset engine. Fuel 2016; 185: 410–420.
[33] Ravi M, Vijaya Kumar KCK, Murugesan A. Certain investigations on the performance of emission, vibration and noise characteristics of C.I engine using bio gas and bio diesel as alternate fuel. International Journal of PharmTech Research 2015; 8: 11–19.
[34] Crocker MJ, Arenas JP. Fundamentals of the direct measurement of sound intensity. Acoustical Physics 2003; 49: 163–175.
[35] Waser MP, Crocker MJ. Introduction to the two-microphone cross-spectral method of determining sound intensity. Noise Control Engineering Journal 1984; 22: 76–85.
[36] Fahy FJ. Measurement of acoustic intensity using the cross-spectral density of two microphone signals. Journal of the Acoustical Society of America 1977; 62: 1057–1059.
[37] Chung JY. Cross-spectral method of measuring acoustic intensity without error caused by instrument phase mismatch. Journal of the Acoustical Society of America 1978; 64: 1613–1616.
[38] Anderton D. Relation between combustion system and engine noise. SAE Technical Papers: 790270; 1979.
[39] Cho SH, Ahn ST, Kim YH. A simple model to estimate the impact force induced by piston slap. Journal of Sound and Vibration 2003; 255: 229–242.
[40] Ohta K, Irie Y, Yamamoto K, et al. Piston slap induced noise and vibration of internal combustion engines (1st Report, Theoretical Analysis and Simulation). SAE Technical Papers: 870990; 1987.
[41] Razak NFD, Sani MSM, Azmi WH, et al. Noise and vibration analysis for automotive radiator cooling fan. IOP Conference Series: Materials Science and Engineering 2017; 257: 012083.
[42] Seifi MR, Hassan-Beygi SR, Ghobadian B, et al. Experimental investigation of a diesel engine power, torque and noise emission using water-diesel emulsions. Fuel 2016; 166: 392–399.
[43] Hassan-beygi SR, Ghobadian B, Kianmehr MH, et al. Prediction of a power tiller sound pressure levels in octave frequency bands using artificial neural networks. International Journal of Agriculture and Biology 2007; 9: 494–498.
[44] Hassan-beygi SR, Ghobadian B, Amiri Chayjan R, et al. Prediction of power tiller noise levels using a back propagation algorithm. Journal of Agriculture Science and Technology 2009; 11: 147–160.
[45] Payri F, Torregrosa AJ, Broatch A, et al. Assessment of diesel combustion noise overall level in transient operation. International Journal of Automotive Technology 2009; 10: 761–769.
[46] Redel-Macías MD, Pinzi S, Leiva D, et al. Air and noise pollution of a diesel engine fueled with olive pomace oil methyl ester and petrodiesel blends. Fuel 2012; 95: 615–621.
[47] Rakopoulos CD, Dimaratos AM, Giakoumis EG, et al. Study of turbocharged diesel engine operation, pollutant emissions and combustion noise radiation during starting with bio-diesel or n-butanol diesel fuel blends. Applied Energy 2011; 88: 3905–3916.
[48] Bezaire N, Wadumesthrige K, Simon Ng KY, et al. Limitations of the use of cetane index for alternative compression ignition engine fuels. Fuel 2010; 89: 3807–3813.
[49] Torregrosa AJ, Broatch A, Novella R, et al. Suitability analysis of advanced diesel combustion concepts for emissions and noise control. Energy 2011; 36: 825–838.
[50] Bayhan Y, Arin S, Kiliç E. Effect of pure biodiesel on fuel injection systems and noise level in agricultural diesel engines. Agricultural Mechanization in Asia Africa and Latin America 2010; 41:78-81.
[51] Redel-Macías MD, Rodríguez-Cantalejo RD, Pinzi S, et al. Evaluation of sound quality in a tractor driver cabin based on the effect of biodiesel fatty acid composition. Fuel 2014; 118: 194–201.
[52] Redel-Macías MD, Pinzi S, Ruz MF, et al. Biodiesel from saturated and monounsaturated fatty acid methyl esters and their influence over noise and air pollution. Fuel 2012; 97: 751–756.
[53] Sadhik Basha J. Impact of carbon nanotubes and di-ethyl ether as additives with biodiesel emulsion fuels in a diesel engine – An experimental investigation. Journal of the Energy Institute 2018; 91: 289–303.
[54] Al-lwayzy SH, Yusaf T. Diesel engine performance and exhaust gas emissions using Microalgae Chlorella protothecoides biodiesel. Renewable Energy 2017; 101: 690–701.
[55] Dykas B, Harris J. Acoustic emission characteristics of a single cylinder diesel generator at various loads and with a failing injector. Mechanical Systems and Signal Processing 2017; 93: 397–414.
[56] Giakoumis EG, Dimaratos AM, Rakopoulos CD. Experimental study of combustion noise radiation during transient turbocharged diesel engine operation. Energy 2011; 36: 4983–4995.
[57] Çelebi K, Uludamar E, Özcanlı M. Evaluation of fuel consumption and vibration characteristic of a compression ignition engine fuelled with high viscosity biodiesel and hydrogen addition. International Journal of Hydrogen Energy 2017; 42: 23379–23388.
[58] Guangpu L, Shihua B, Hongxia P. Analysis of noise characteristics for diesel engine. In: Proceedings of IEEE ICIA 2006 - 2006 IEEE International Conference on Information Acquisition, Veihai, China, pp. 1390–1394; 2006.
[59] Jaikumar S, Bhatti SK, Srinivas V, et al. Combustion and vibration characteristics of variable compression ratio direct injection

diesel engine fuelled with diesel-biodiesel and alcohol blends. Engineering Reports 2020; 2: 1–11.
[60] Geng L, Chen Y, Chen X, et al. Study on combustion characteristics and particulate emissions of a common-rail diesel engine fueled with n-butanol and waste cooking oil blends. Journal of the Energy Institute 2019; 92: 438–449.
[61] Satsangi DP, Tiwari N. Experimental investigation on combustion, noise, vibrations, performance and emissions characteristics of diesel/n-butanol blends driven genset engine. Fuel 2018; 221: 44–60.